buildings

MDPI

Article

Effect of Relative Density on the Lateral Response of Piled Raft Foundation: An Experimental Study

Mohammad Ilyas Siddiqi [1], Hamza Ahmad Qureshi [2], Irfan Jamil [1] and Fahad Alshawmar [3,*]

[1] Department of Civil Engineering, University of Engineering and Technology, Peshawar 25000, Pakistan; ilyas.siddiqi@uetpeshawar.edu.pk (M.I.S.); engrirfan@uetpeshawar.edu.pk (I.J.)
[2] Department of Civil Engineering, Ghulam Ishaq Khan Institute of Engineering Sciences and Technology, Topi 23640, Pakistan; hamza.ahmad@giki.edu.pk
[3] Department of Civil Engineering, College of Engineering, Qassim University, Buraydah 51452, Saudi Arabia
* Correspondence: shomr@qu.edu.sa

Abstract: The population surge has led to a corresponding increase in the demand for high-rise buildings, bridges, and other heavy structures. In addition to gravity loads, these structures must withstand lateral loads from earthquakes, wind, ships, vehicles, etc. A piled raft foundation (PRF) has emerged as the most favored system for high-rise buildings due to its ability to resist lateral loads. An experimental study was conducted on three different piled raft model configurations with three different relative densities (D_r) to determine the effect of D_r on the lateral response of a PRF. A model raft was constructed using a 25 mm thick aluminum plate with dimensions of 304.8 mm × 304.8 mm, and galvanized iron (GI) pipes, each 457.2 mm in length, were used to represent the piles. The lateral and vertical load cells were connected to measure the applied loads. It was found that an increase in D_r increased the soil stiffness and led to a decrease in the lateral displacement for all three PRF models. Additionally, the contribution of the piles in resisting the lateral load decreased, whereas the contribution of the raft portion in resisting the lateral load increased. With an increase in D_r from 30% to 90%, the percentage contribution of the raft increased from 42% to 66% for 2PRF, 38% to 61% for 4PRF, and 46% to 70% for 6PRF.

Keywords: soil; particle size; classification; piled raft foundation; relative density; dynamic cone penetrometer; lateral load; stress; strain gauge

Citation: Siddiqi, M.I.; Qureshi, H.A.; Jamil, I.; Alshawmar, F. Effect of Relative Density on the Lateral Response of Piled Raft Foundation: An Experimental Study. *Buildings* **2024**, *14*, 3687. https://doi.org/10.3390/buildings14113687

Academic Editor: Fabrizio Gara

Received: 10 October 2024
Revised: 14 November 2024
Accepted: 16 November 2024
Published: 19 November 2024

1. Introduction

The foundation is the most critical part of any structure because of its ability to provide support and stability to ensure the long-term integrity of the structure. For cohesionless and expansive soils, the shallow foundations cannot sustain the heavy lateral loads, and piles are essential for providing stability and load-bearing support in such conditions. Properly designed deep foundations can adapt to expansive soil conditions, by adjusting the pile length and diameter. Longer piles that exceed the thickness of the active zone are more effective in resisting volumetric changes. Granular anchor piles are significantly more effective than concrete piles in highly expansive soil conditions. Specifically, they perform over 50% better in terms of mitigating the adverse effects caused by soil expansion [1]. Pile foundations reinforce embankments and retaining structures to ensure slope stability and reduce the soil arching effect [2]. The shape of the pile cap can affect the load efficiency of a pile and the settlement of an embankment [3]. Utilizing longer and capped piles significantly decreases both the maximum and differential settlements [3].

Shallow foundations such as rafts and deep foundations such as piles were used separately. However, geotechnical engineers have started to combine these two systems. By integrating them, engineers can achieve the required safety values for design while also providing a more economical solution in the form of pile group and piled raft foundation [4–6].

The piled raft foundation (PRF) and pile group foundation both consist of piles and rafts, but the main difference between them is that in the pile group foundation, there is a free space between the raft and ground surface, whereas in the case of a PRF, the raft is in contact with the soil, and there is no gap between the raft and the supporting soil. Because of this contact, the interaction between the raft and soil is considered during the PRF design. Many researchers [7–10] have explored the foundation design for high-rise buildings with a preference for a PRF because of its economical and safety features. PRFs have been used in marine and offshore structures [11–14]. The concept of a PRF was initially introduced by Zeevaert in 1957 [15]. He used the PRF system for "Tower Latino Americana" in Mexico. The PRF has been divided into two categories by [16]: small PRFs, which are those with a raft width-to-pile length ratio of less than 1, while for large PRFs, the raft width is greater than the length of the pile. In a small PRF, the provision of piles increases the bearing capacity and reduces the settlement of the foundation, whereas in a large PRF, the raft typically offers sufficient bearing capacity, and the provision of piles is used to control the total and differential settlement [16]. The lateral resistance of a PRF is approximately 2.5 to 6 times greater than that of pile group foundations with the same configuration [17]. The primary advantage of a PRF over the conventional pile group foundation is its ability to resist lateral loads; according to [18], the raft can resist 21–81 percent of the total vertical load and 15–61 percent of the total applied lateral load on the PRF. In a pile group foundation, it is assumed that the raft does not contribute to the resistance of the lateral load [19,20]. In a PRF, the piles provide the necessary support for the structure and are used as settlement reducers [21], whereas the raft reduces the bearing pressure by distributing the load over the supported soil [22]. The use of piles at strategic locations improves the bearing capacity of the raft portion in a PRF [23]. The length of the piles does not significantly impact the load sharing mechanism of a PRF [24]. With the increase in the raft–soil relative stiffness, the differential settlement of the PRF decreases [25]. Several researchers have studied the contribution of the vertical load among the piles and raft in a PRF [26–28], but very limited research has been conducted on the lateral load sharing behavior in a PRF. Jamil et al. [29] conducted an experimental and numerical study to examine various parameters affecting the lateral load contribution of a raft in a piled raft foundation system. The study concluded that the vertical pressure is directly related to the raft's lateral load contribution, whereas the pile length, the number of piles, and the spacing-to-diameter ratio are inversely related. According to Plaban Deb and S.K Pal [30], the lateral load capacity of a PRF increases with the application of a vertical load. Increasing the vertical load also enhances the lateral load capacity of the raft. For spacing between the piles and diameter of pile ratios ranging from 3 to 5, the lateral load capacity of both the pile and raft increased by approximately 14–25%. A numerical study was conducted by [31] on the lateral response of a PRF and found that at the initial stage of loading, approximately 85% of the total lateral load was taken as the raft portion. In a PRF with a rigid pile head connection, a higher lateral load is transferred to the piles, resulting in greater initial horizontal stiffness than a PRF with a hinged connection [32].

In the literature, numerous researchers have investigated the load sharing behavior of a PRF and the various factors influencing it. However, the impact of the soil density on the load sharing behavior of a PRF remains unclear. Therefore, a detailed experimental investigation was carried out by using small-scale piled raft models. This research aims to explore the effect of the relative density (D_r) on the lateral response of a PRF through a detailed experimental study. It focuses on evaluating how changes in D_r influence the load sharing behavior between the raft and pile elements of a PRF. The findings seek to offer valuable insights for optimizing PRF designs to enhance the lateral load resistance in high-rise structures.

2. Materials and Methods

2.1. Soil Sample

Locally sourced clean dry sand was used as the test medium. To determine its geotechnical properties, all necessary tests were carried out according to the ASTM standards. Sieve analysis was performed for the gradation of the soil sample (ASTM D-6913) [33]. Figure 1 displays the curve representing the particle-size distribution of the soil. From Figure 1, it can be concluded that the soil is poorly graded sand (SP), according to the Unified Soil Classification System (USCS).

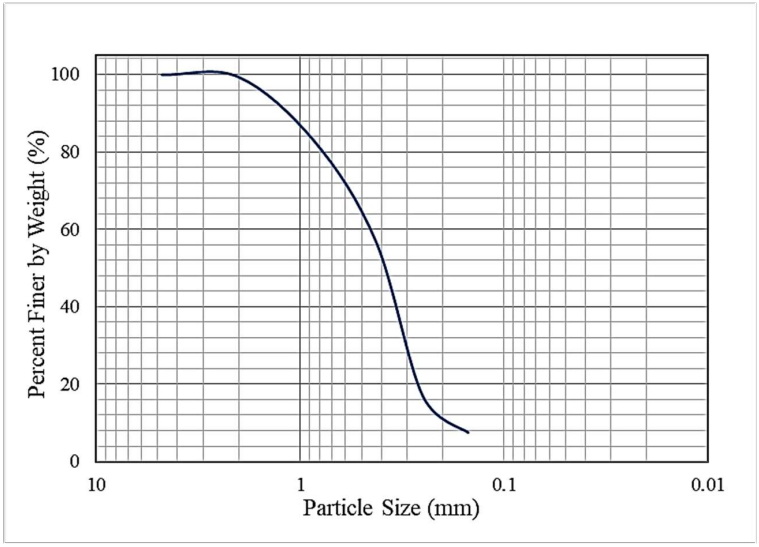

Figure 1. Particle size distribution of the soil used in this study.

Direct shear tests were performed on loose, medium, and dense sand (D_r 30%, D_r 60% and D_r 90% respectively) in order to determine the angle of internal friction as shown in Figures 2–4 respectively.

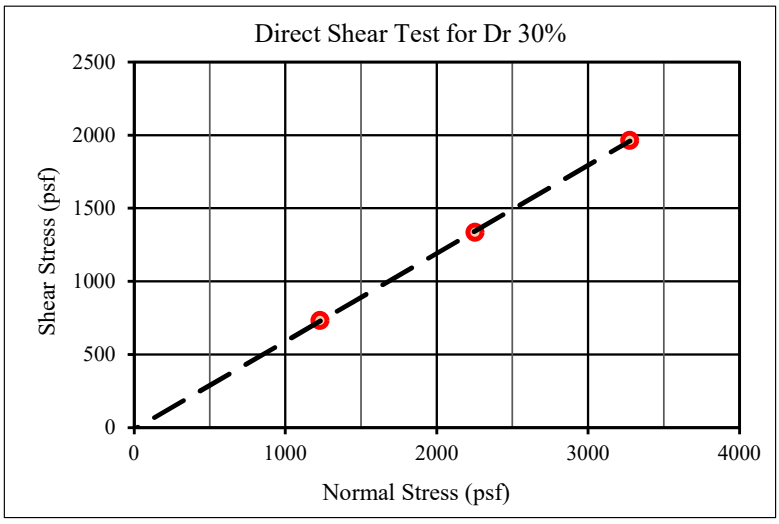

Figure 2. Direct shear test results for D_r 30%.

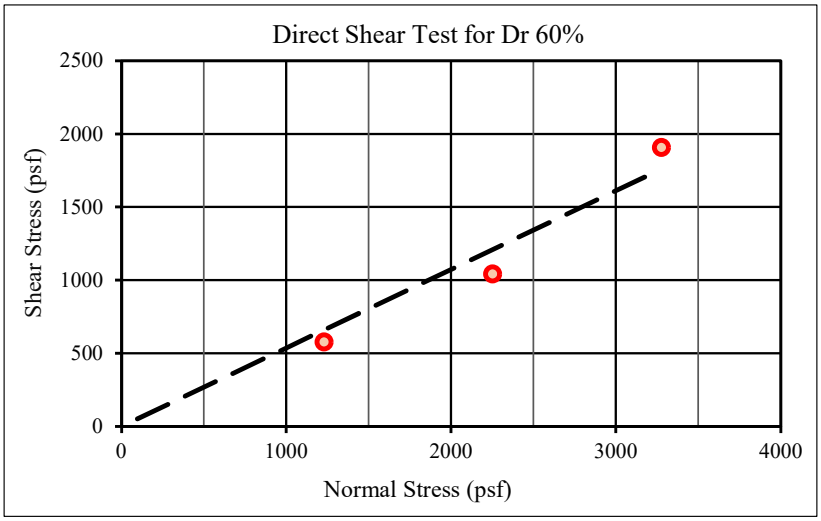

Figure 3. Direct shear test results for Dr 60%.

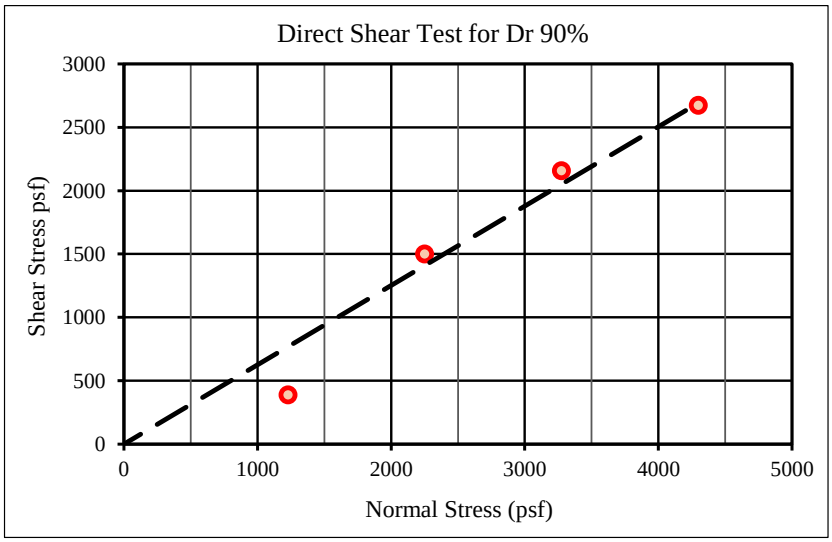

Figure 4. Direct shear test results for Dr 90%.

The maximum and minimum dry unit weights of the soil samples were calculated to determine their relative densities. Equation (1) was used to obtain the relative densities of 30%, 60%, and 90% [34]. Table 1 tabulates the geotechnical properties of the sand used in this study.

$$D_r(\%) = \left(\frac{\gamma_d - \gamma_{min}}{\gamma_{max} - \gamma_{min}}\right) * \left(\frac{\gamma_{max}}{\gamma_d}\right) \quad (1)$$

Table 1. Soil properties.

Tests Performed	ASTM Standards	Property	Value
Sieve analysis	ASTM D-6913	D_{10}	0.175 mm
		D_{30}	0.307 mm
		D_{50}	0.394 mm
		D_{60}	0.474 mm
		Coefficient of gradation (C_c)	1.136
		Coefficient of uniformity (C_u)	2.708

Table 1. *Cont.*

Tests Performed	ASTM Standards	Property	Value
Maximum and minimum dry unit weights	ASTM D-4253 [35] ASTM D-4254 [36]	$\gamma_{d\ max}$ $\gamma_{d\ min}$	17.058 (kN/m^3) 13.890 (kN/m^3)
Specific gravity	ASTMD-854 [37]	G_s	2.65
Direct shear test	ASTM D-3080 [38]	Frictional angle, φ' for D_r 30%	31°
		Frictional angle, φ' for D_r 60%	33°
		Frictional angle, φ' for D_r 90%	36.3°

2.2. Model Soil Box

The selection of the soil box dimensions is a crucial factor for ensuring that the soil stress remains within the selected boundary. Unsever [31] used a lateral boundary of 3.33 times the width of the raft (W_r), and the vertical boundary was approximately twice the embedded length of the pile (L_p) for the lateral load analysis of the PRF. Similarly, Katzenbach [39] used a lateral boundary of 3.57 W_r and vertical boundary of 1.93 L_p. To satisfy the boundary conditions, a model soil box with dimensions of 1.2 m in length, 0.9 m in width, and 1.5 m in height was used as a model soil box. The dimensions of the soil box were such that the width of the testing tank was 3 times W_r, and the height of the tank was 3.33 times L_p. A model soil box with stiffeners and a 3D view are shown in Figure 5.

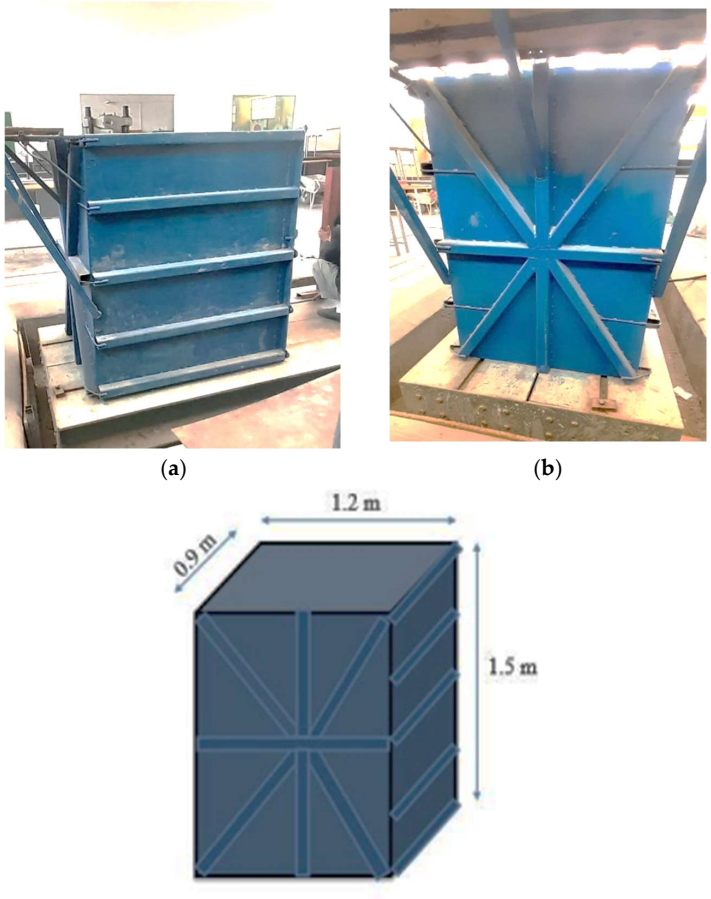

(**a**) (**b**)

(**c**)

Figure 5. (**a**) Model soil box; (**b**) horizontal and diagonal stiffeners; (**c**) 3D view of the box.

2.3. Model Raft and Piles

A square (304 mm × 304 mm) aluminum plate with a thickness of 25 mm was used as the model raft (Figure 6). A hook was connected to the raft to apply lateral load. In addition, 20 mm holes were created in the raft for piles and raft rigid connections. Galvanized hollow iron pipes with an outer diameter of 19.05 mm, an internal diameter of 16.70 mm, and a length of 457 mm were employed as model piles. These hollow pipes were used owing to their sensitivity to small strains [4]. The toe of the piles was closed by steel plates, and a plain bar with a 19 mm diameter was used for the pile and raft connection, as shown in Figure 7.

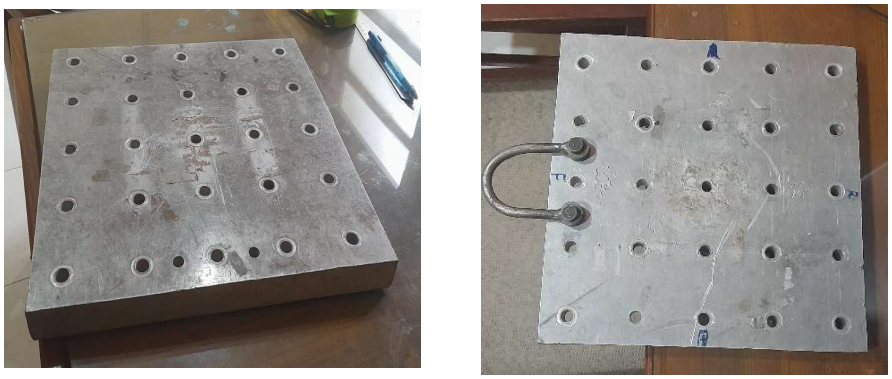

(**a**) (**b**)

Figure 6. (**a**) Model raft; (**b**) raft with hook.

Figure 7. Model piles.

2.4. Piled Raft Configurations

Three different configurations, namely 2 × 1, 2 × 2, and 2 × 3, were employed in this study. The spacing between the piles was kept constant for all three models (127 mm). The piles were connected precisely in a vertical position throughout the depth of the PRF to ensure uniform spacing between them. For a rigid connection, the piles were fitted into the holes of 25 mm thick aluminum raft through nuts. The top views of the schematic diagrams of the models and the real PRF models are shown in Figures 8 and 9, respectively.

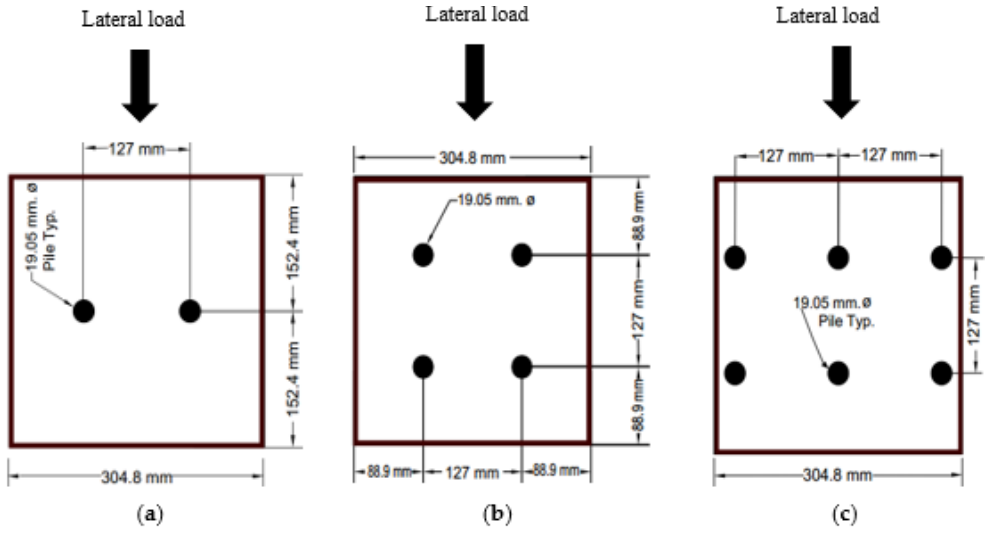

Figure 8. Top view schematic diagram of: (**a**) 2PRF; (**b**) 4PRF; (**c**) 6PRF.

(**a**) (**b**) (**c**)

Figure 9. Real PRF models: (**a**) 2PRF; (**b**) 4PRF; (**c**) 6PRF.

2.5. Strain Gauge Installation

Shear strain gauges were attached to each pile to act as load cells for measuring the lateral loads transferred from the raft to the piles. Each strain gauge, with a gauge length of 7 mm and resistance of 350 Ω, was capable of measuring the strain with a precision of 1 μm/m. Prior to installing the strain gauges, the surfaces of the model piles were smoothed with coarse sandpaper to remove major fractures or grooves. To remove fine particles, alcohol and other recommended solvents [40] were used. The precise location of the strain gauge on the pile was demarcated with a pencil, and the strain gauge was affixed to the pile using epoxy.

A Wheatstone bridge configuration was employed as the load cell, incorporating four strain gauges into a single cell. As shown in Figure 10, these strain gauges were located 25 mm beneath the pile head, with two tension gauges on one side and two compression gauges on the other side. These strain gauges were installed such that all were perpendicular to the direction of the applied lateral load. These load cells were tested using an ammeter and subjected to an initial calibration process to ensure accurate lateral load measurements.

Figure 10. Strain gauge installation.

2.6. Strain Gauge Calibration

Proper calibration is critical to ensure accuracy in data collection. Therefore, an initial calibration process was undertaken to ensure the strain gauge accuracy. A digital balance was attached to the steel rope near the pile to measure the accurate load transfer, as shown in Figure 11. Incremental loads ranging from 9.8 N to 980 N were applied, and the corresponding strain gauge readings were recorded. To determine the calibration factor, these readings were divided by the respective loads. The calibration factors remained consistent across all increments, which allowed the calibration process to be concluded at a load of 980 N for each pile. Table 2 shows the calibration factors for each pile.

(**a**) (**b**)

Figure 11. Strain gauge calibration process. (**a**) Digital balance. (**b**) Load arrangement for calibration.

Table 2. Calibration factors for 9.8 N load.

Pile Name	Pile 1	Pile 2	Pile 3	Pile 4	Pile 5	Pile 6
Calibration factor	3.3	3.5	3.5	3.8	3.3	3.5

2.7. Preparation of Testing Medium

The arrangement and packing of sand grains significantly affected the load settlement behavior of the PRF. Consequently, a methodology for creating a sand bed with uniform density was required [28]. A mobile pluviator or sand raining technique was employed to achieve uniform density in the soil box. This technique has been successfully used by numerous researchers [29,34,41,42]. As the density of sand is dependent on the height of the fall and the sand particles, several tests were conducted to determine the relationship between the relative density (D_r) and the height of the fall for the sand used in this study, as shown in Figure 12.

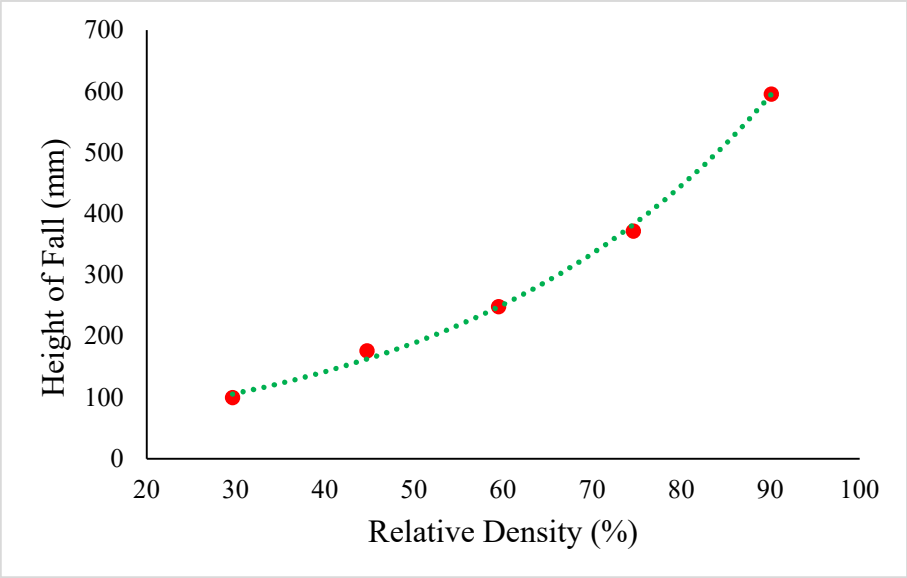

Figure 12. Variation in relative density with free fall height.

After preparing the test medium, the density of the sand was verified using both the weight–volume relationship and a small dynamic cone penetrometer (DCP). The dynamic cone penetrometer was chosen for its simplicity, cost-effectiveness, and efficiency in providing rapid in situ measurements. Various correlations are available to estimate the soil properties from the cone resistance [43]. To obtain more precise results, DCP tests were conducted at all four corners and at the center of the soil box. The DCP test results and positions are shown in Figure 13.

(**a**) (**b**)

Figure 13. (**a**) Verification of D_r with DCP; (**b**) positions for performing DCP.

To verify the density, the penetration of the cone was recorded in centimeters per blow (cm/blow). Upon completion of each test, readings were taken, and the corresponding density was calculated using the correlation presented in [44].

$$D_r(\%) = \frac{189.93}{DPI^{0.53}} \quad (2)$$

where DPI is the dynamic penetration index.

It was observed that the DCP provided accurate results for the dense sand. However, the results were less accurate for the loose sand. Comparison curves of D_r 60% and D_r 90% are given in Figure 14.

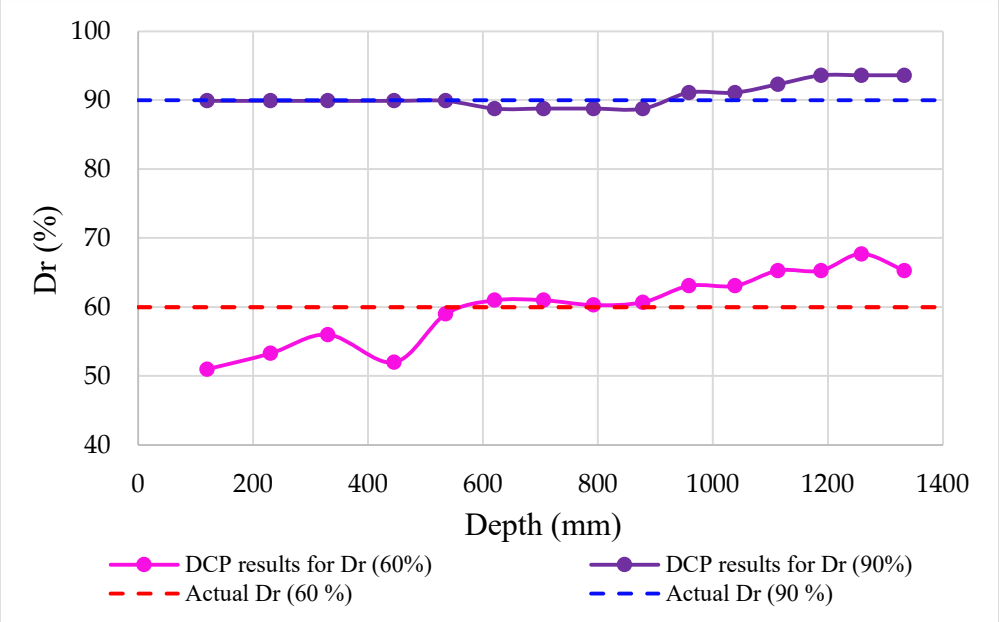

Figure 14. Comparison curve for DCP results.

3. Test Procedure

A step-by-step procedure is outlined below:

- The model box was filled to a height of 1.07 m (corresponding to the pile tips) using the sand raining technique as described earlier. Once this level was reached, the model was precisely positioned at the center of the box.
- The box was then filled to two-thirds of the pile length.
- The raft was carefully removed without disturbing the pile positions, and the soil box was filled to the final level.
- The raft was installed over the piles using a long-handled wrench to maintain the orientation and position of the piles, creating a non-displacement piled raft.
- Supporting plates with sufficient rigidity and thickness were placed beneath the vertical load cell to ensure a uniformly distributed vertical load and prevent stress concentration at any single point.
- Linear variable displacement transducers (LVDTs) were installed in the overall system to measure the lateral displacement resulting from the applied lateral load.
- The LVDTs, along with the lateral, vertical, and pile load cells, were connected to a data logger for data acquisition.
- A hydraulic loading jack was used to apply a vertical load, and this load was maintained until the experiment concluded.
- A lateral load was applied through a hydraulic machine with a capacity of 5 tons, equipped with a lateral load cell at the front of the hydraulic jack, by utilizing a hook arrangement for the application of the lateral load.

- The loading and unloading processes were regulated using the control lever on the machine, and the rate of load application by the hydraulic pumps was maintained at a very low rate, approximately 4.9 N/s (0.5 kg/s), to allow for the collection of the lateral displacement values resulting from very small lateral loads.
- Data were collected from the data logger for further analysis. A schematic diagram is shown in Figure 15.

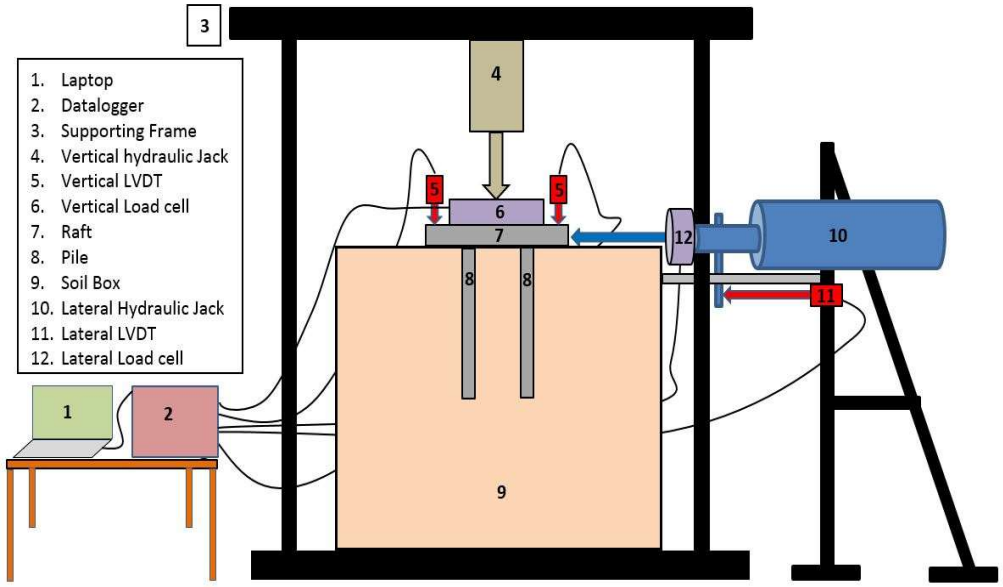

Figure 15. Schematic diagram of test setup.

The experimental instruments used during this study are shown in Figure 16, and the overall vertical and lateral load setups are shown in Figures 17 and 18, respectively.

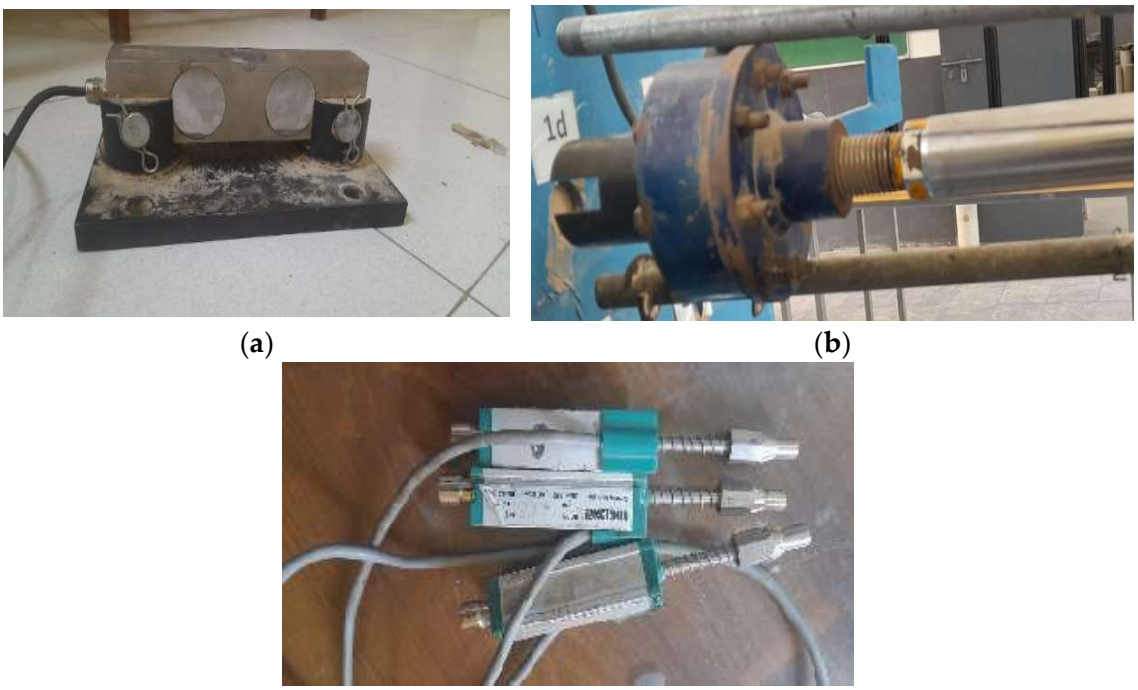

(**a**) (**b**)

(**c**)

Figure 16. (**a**) Vertical load cell; (**b**) lateral load cell; (**c**) LVDTs.

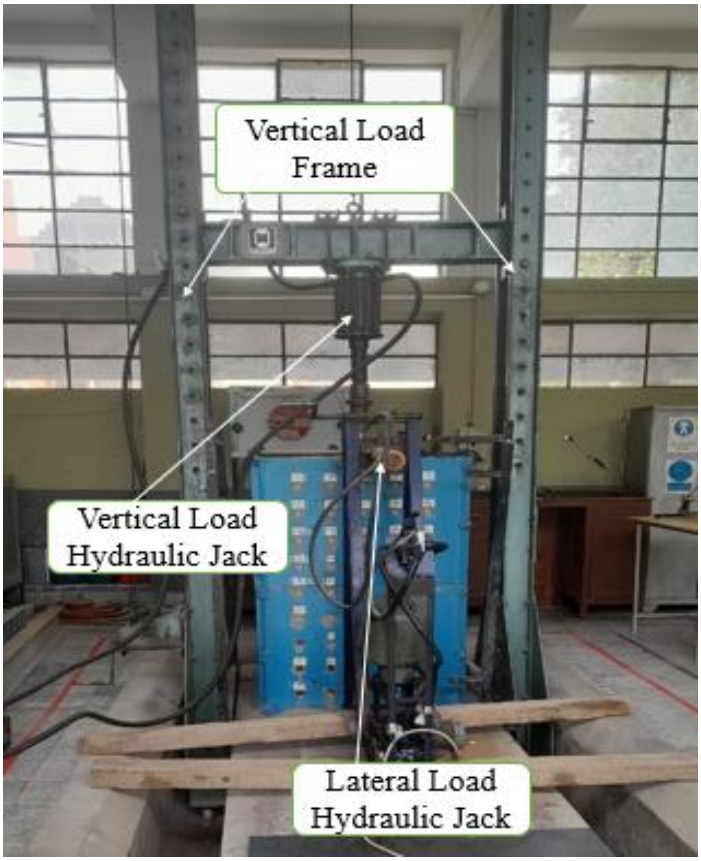

Figure 17. Vertical load setup.

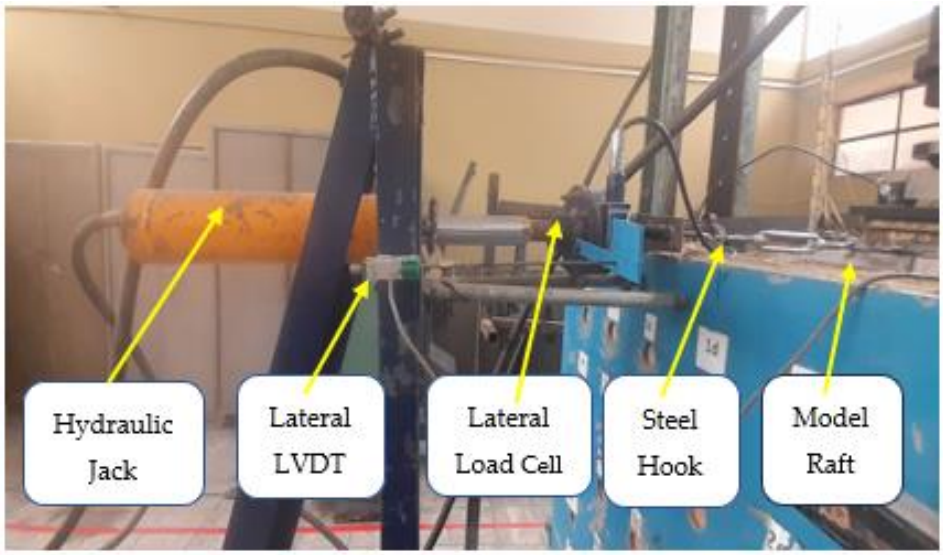

Figure 18. Lateral load setup.

4. Results and Discussion

A total of 27 tests were conducted, as listed in Table 3. Each test was conducted three times to minimize the experimental errors, and the average values were used as the final results. Tests with errors exceeding 5% were excluded. A static vertical load of 6 kN was applied for the lateral load analysis of all three configurations. Although this research focused only on the lateral load analysis of the PRF, to simulate a real-world scenario, a

lateral load analysis was conducted under the application of vertical loads. Subsequently, a hydraulic jack was used to apply lateral load, and all readings were recorded.

Table 3. Tests conducted.

Classification	Relative Density (%)	PRF Configuration	No. of Tests
Loose	30%	2, 4, 6	3
Medium	60%	2, 4, 6	3
Dense	90%	2, 4, 6	3

4.1. Effect of Relative Density on 2PRF

A model with two piled raft configurations was analyzed in sand with D_r values of 30%, 60%, and 90%, as shown in Figures 19–21, respectively. For D_r 30%, as shown in Figure 19, initially up to a 180 N lateral load, when there was no displacement in the PRF, the raft portion played a significant role in resisting the lateral load, contributing more than the piles. However, once the raft portion began to displace, its load-carrying capacity decreased rapidly, while the contribution of the piles started to increase. After a displacement of 2.8 mm, the raft contact stiffness reduced, leading to a state in which the piles began to resist more load than the raft. This transition indicated that the role of the pile became critical after this displacement. As the D_r increased to 60% and 90%, it enhanced the contact pressure between the raft and the soil, leading to a larger portion of the load being resisted by the raft compared to D_r 30%. This meant that at higher densities (D_r 60% and 90%), the raft could withstand more lateral loads before the piles started to contribute.

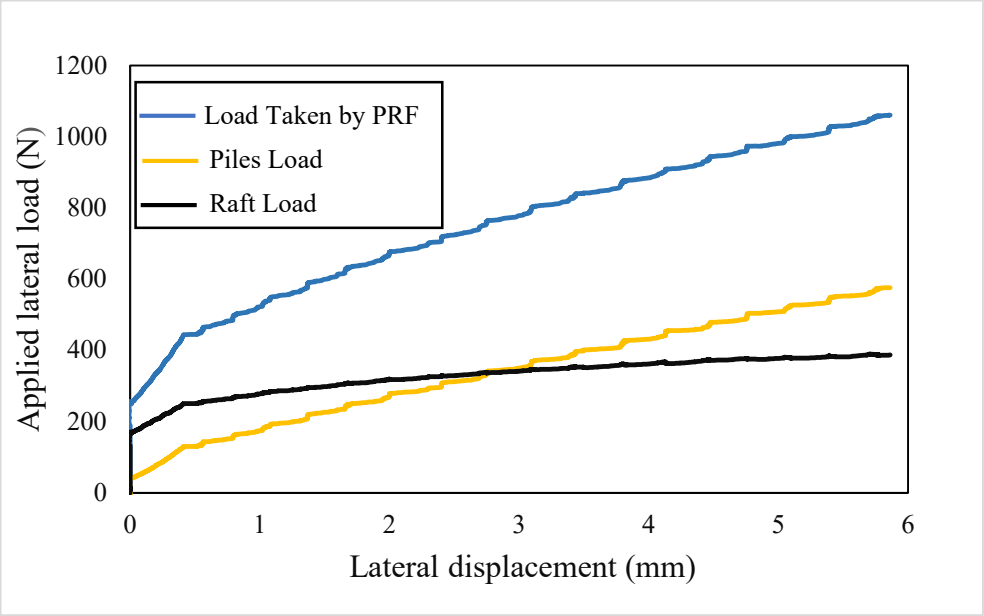

Figure 19. Analysis of 2PRF at D_r 30%.

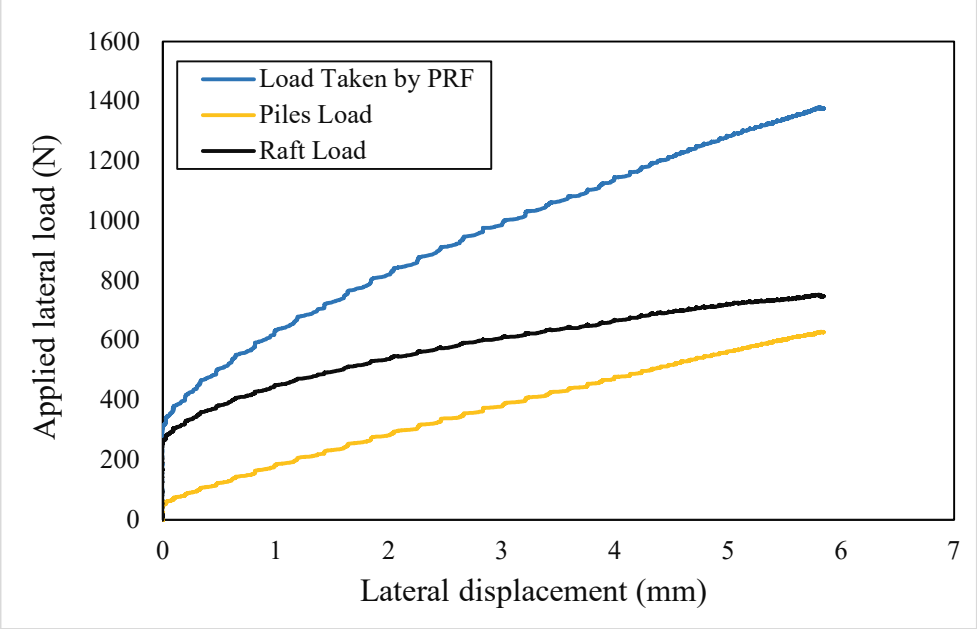

Figure 20. Analysis of 2PRF at D_r 60%.

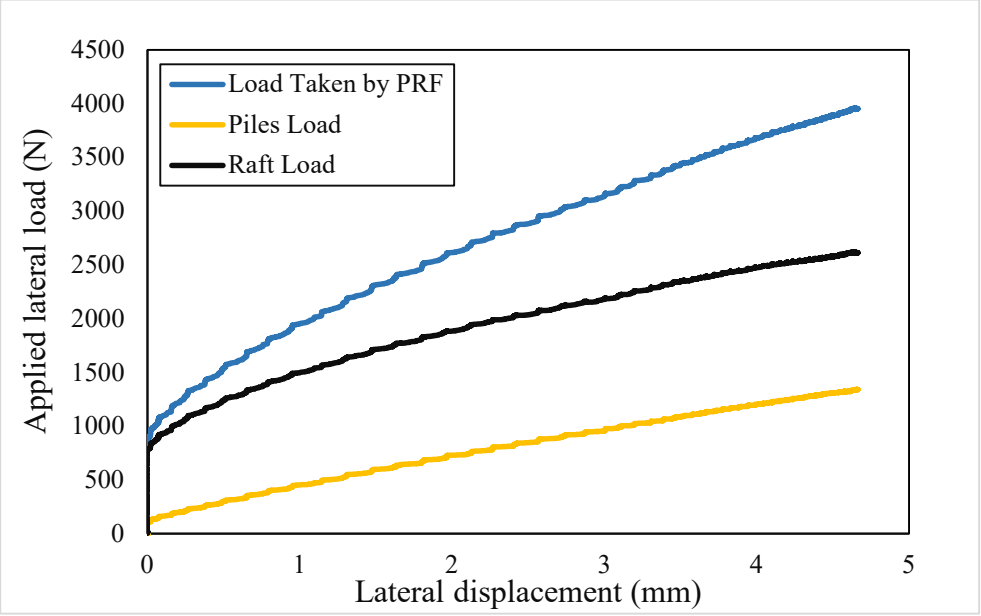

Figure 21. Analysis of 2PRF at D_r 90%.

4.2. Effect of Relative Density on 4PRF

The results for 4PRF at D_r 30% and 60% and 90% are shown in Figures 22–24 respectively. With the increase in the number of piles, the contact pressure between the raft and soil decreased. Initially, upon the application of the lateral load, the contributions of the raft and piles were approximately the same; however, as the lateral load increased, leading to greater displacement, the contribution of the raft in resisting the lateral load decreased significantly. In contrast, the piles displayed a nearly linear response to the displacement. This distinction arises because the resistance of the raft is primarily due to interface friction, whereas the piles provide resistance along their entire length.

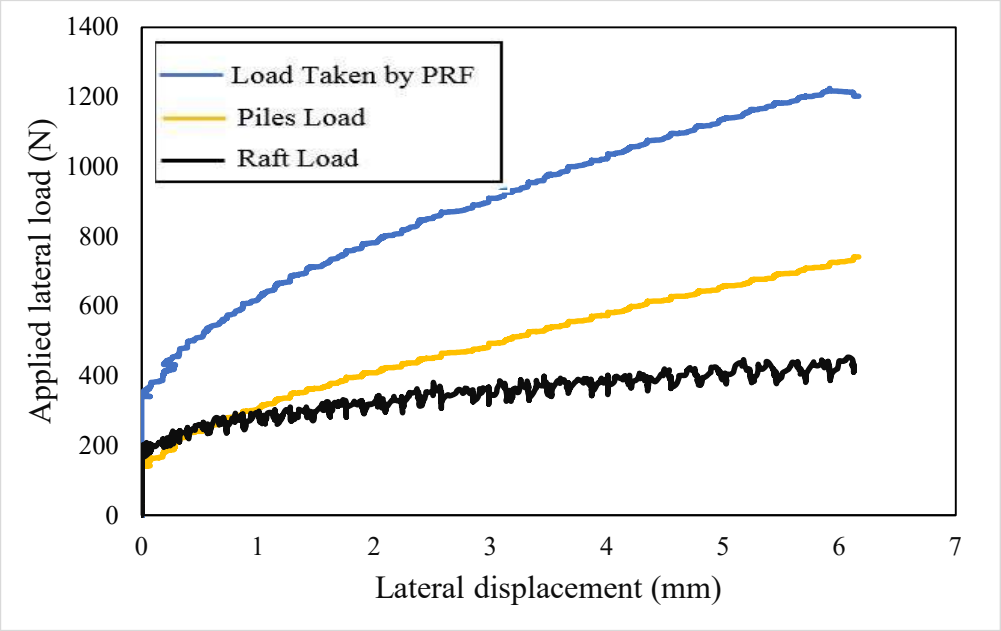

Figure 22. Analysis of 4PRF at D_r 30%.

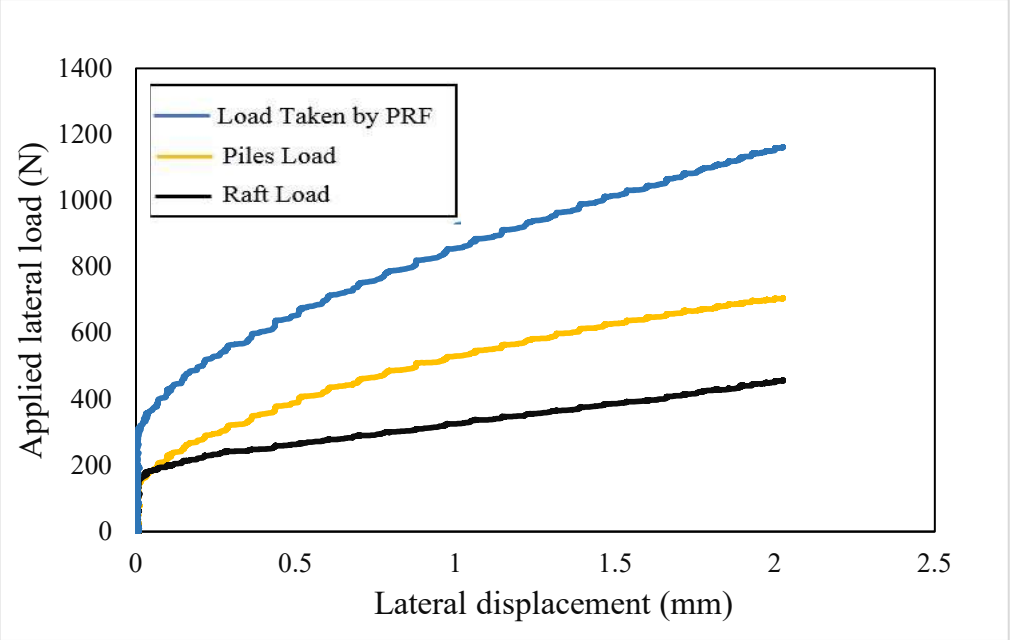

Figure 23. Analysis of 4PRF at D_r 60%.

The lateral load contribution of the piles decreased for D_r 90%, while the contribution of the raft portion in resisting the lateral load increased, as shown in Figure 24. The lateral load sharing by the piles and raft depended on the lateral displacement. Initially, the raft components shared the total lateral load. As loading progressed and the raft's resistance was fully mobilized, the piles began to take on the lateral load, increasing their load sharing role at larger displacements.

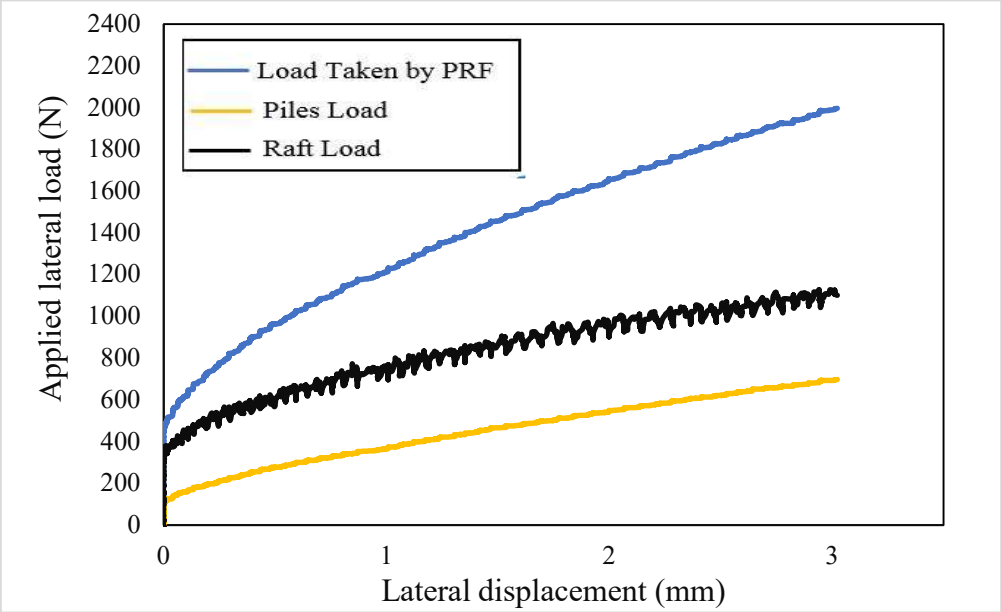

Figure 24. Analysis of 4PRF at D_r 90%.

4.3. Effect of Relative Density on 6PRF

For 6PRF, as the number of piles increased, their contribution to the total lateral load also increased. Figure 25 shows the load sharing between the piles and raft under a D_r of 30%. Initially, the lateral load was carried by the raft only, but after some displacement occurred, the piles also contributed to resisting the lateral load. The contribution of the piles increased as the displacement increased, whereas that of the raft decreased.

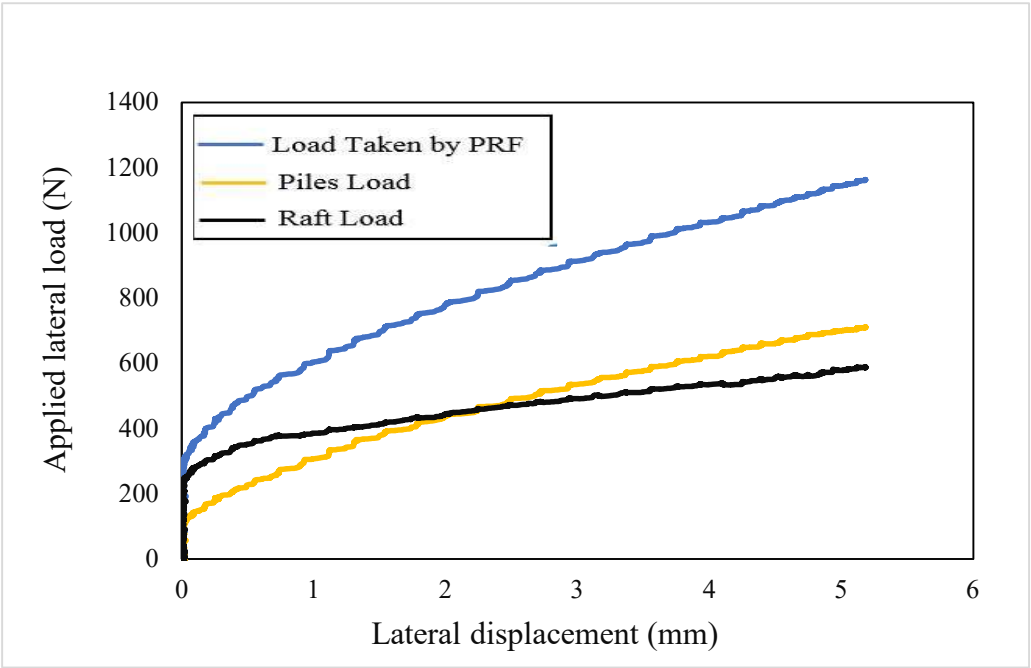

Figure 25. Analysis of 6PRF at D_r 30%.

The lateral load behavior of 6PRF at 60% relative density is shown in Figure 26. In this case, the load-carrying capacity of the raft increased compared to that at the lower D_r. The raft revealed the ability to sustain a higher load before significant displacement occurred. However, the load-carrying capacity of the piles decreased relative to that of the raft.

This behavior suggests that the increased soil density enhanced the raft interaction with the soil, thereby improving its ability to resist lateral loads more effectively.

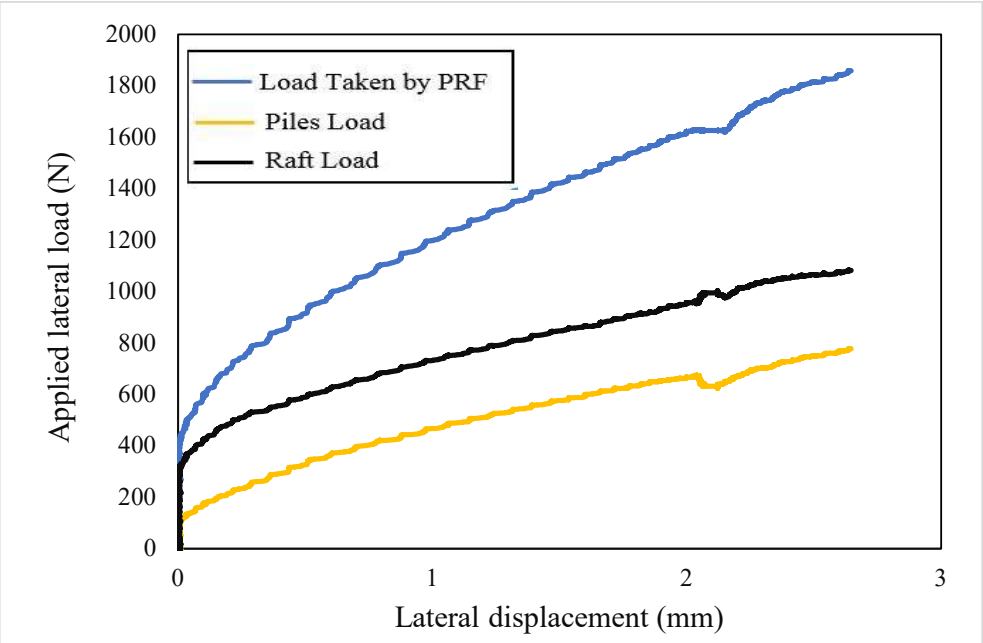

Figure 26. Analysis of 6PRF at D_r 60%.

For the 6PRF configuration at 90% D_r, as shown in Figure 27, the trend continued as the load-carrying capacity of the raft increased further. The raft was capable of resisting a substantial portion of the lateral load before noticeable displacement occurred. The piles, while still contributing to the load resistance, carried less load compared to the raft as D_r increased. This indicates that higher relative densities significantly improve the raft's effectiveness in terms of lateral load resistance, reducing the dependency on the piles.

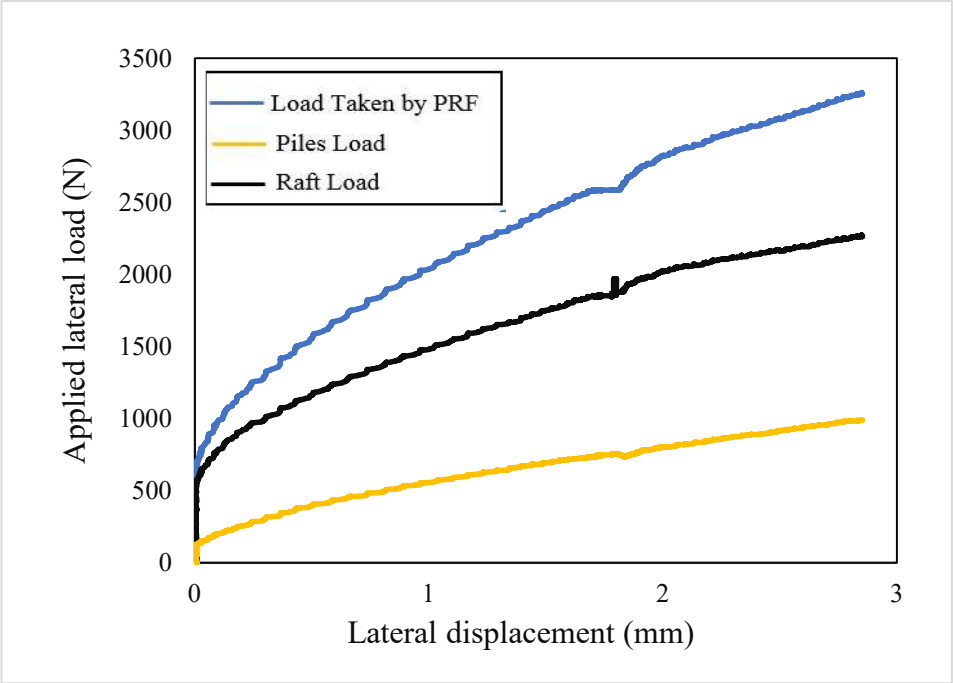

Figure 27. Analysis of 6PRF at Dr 90%.

4.4. Percentage Contribution of Piles and Raft

Based on the maximum displacement, the percentage contribution of the piles and raft portions was analyzed against the relative density for all configurations. The analysis revealed that with an increase in D_r from 30% to 90%, the percentage contribution of the raft increased from 42% to 66% for 2PRF, from 38% to 61% for 4PRF, and from 46% to 70% for 6PRF, as shown in Figures 28–30 respectively. The analysis revealed that the percentage contribution of the piles decreased as D_r increased.

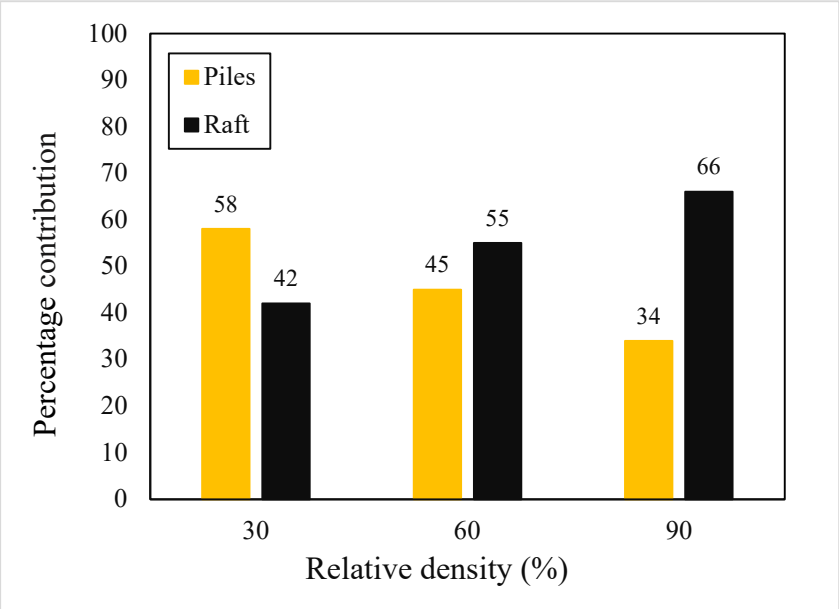

Figure 28. Percentage contribution of 2PRF.

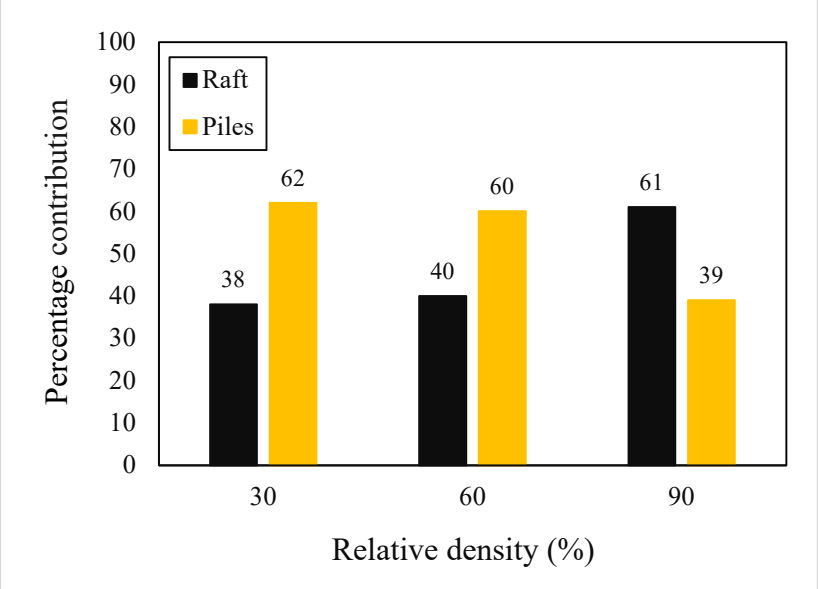

Figure 29. Percentage contribution of 4PRF.

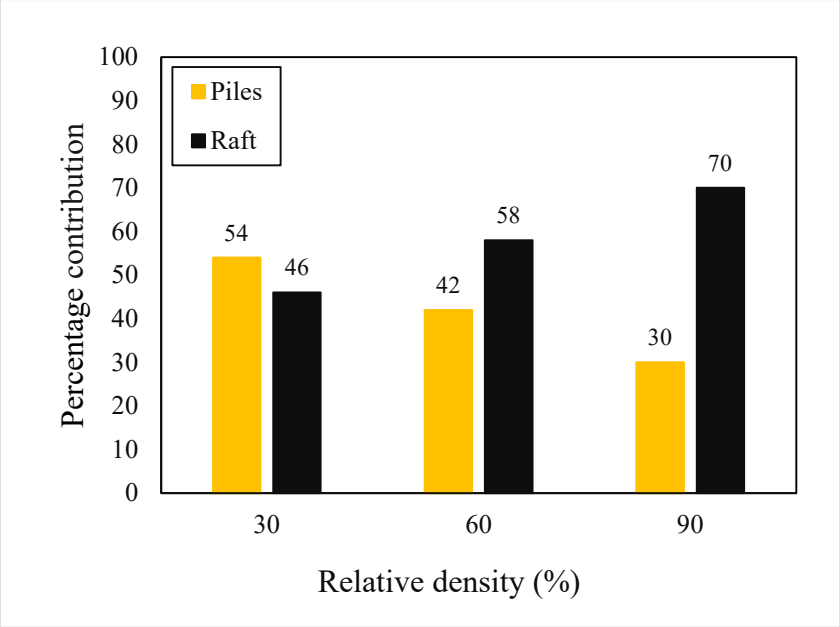

Figure 30. Percentage contribution of 6PRF.

Table 4 presents the percentage contribution of the model piles and raft at lateral displacements of 0.5 mm and 1 mm.

Table 4. Percentage contribution of piles and raft at 0.5 mm and 1 mm lateral displacement.

Relative Density (%)	Lateral Displacement		% Contribution		
			2PRF	4PRF	6PRF
30	0.5 mm	Piles	34	50	39
		Raft	66	50	61
	1 mm	Piles	38	52	44
		Raft	62	48	56
60	0.5 mm	Piles	24	60	36
		Raft	76	40	64
	1 mm	Piles	29	62	39
		Raft	71	38	61
90	0.5 mm	Piles	20	33	25
		Raft	80	67	75
	1 mm	Piles	23	35	27
		Raft	77	65	73

5. Conclusions

From the results obtained in this study, the following conclusions were made.

- The performance of a piled raft foundation (PRF) in resisting the lateral load is greatly reliant on the density of the surrounding soil. As the relative density (D_r) increases, the soil stiffness increases, and as a result the lateral displacement for all PRF models decreases.
- Initially, when a lateral load is applied to the PRF, the raft portion resists all lateral loads, preventing any lateral displacement. However, as the lateral load increases, the displacement of the PRF also increases, causing the raft to gradually transfer load to the

piles. This load transfer occurred because of the rigid connection between the pile and raft, which allows the raft to transfer some of the load to the piles. Consequently, the contribution of the raft in resisting the lateral load decreases, whereas the contribution of piles in resisting the lateral load increases with further lateral displacement.

- In loose soils, the lateral load is primarily resisted by the piles because of the reduced contact pressure between the raft and adjacent soil. As D_r increases from the loose to dense state, the raft becomes more effective in resisting lateral loads, and the contribution of the raft portion to resist the lateral load increases, while the contribution of the piles in resisting the lateral load decreases; that is, with an increase in D_r from 30 to 90%, the percentage contribution of the raft increased from 42% to 66% for 2PRF, 38% to 61% for 4PRF, and 46% to 70% for 6PRF.
- The contribution of the piles to resist the lateral load decreases with an increase in D_r; that is, with an increase in D_r from 30 to 90%, the percentage contribution of the piles decreases from 58% to 34% for 2PRF, 62% to 39% for 4PRF, and 54% to 30% for 6PRF.
- At lower densities and large displacements, piles play a crucial role in resisting lateral loads. For dense soils, the raft becomes more effective in resisting the initial applied load.
- A small dynamic cone penetrometer (DCP) apparatus provides good results for dense sands compared to loosen sands.

6. Practical Applications

Relative density is a very important parameter in the analysis of a PRF, as the D_r affects the pile's lateral load distribution, the lateral load contribution of piles and raft, and lateral deflection of a PRF. So, for the practical design of a PRF, the effect of D_r should not be ignored.

Based on the findings of this study, practical applications are given below:

- For dense soils, the raft portion of a PRF becomes more critical and requires careful attention during the design stage.
- In loose soils, where there is a greater likelihood of larger lateral displacements, piles become more critical. Engineers should therefore pay special attention to the design of piles when working with such soil types.

7. Future Recommendations

- This research could be extended to investigate the response of a PRF under dynamic cyclic loading conditions to better understand the behavior under real-world scenarios such as earthquakes and traffic loads.
- This research could be expanded to examine the response of a PRF in layered soil profiles.
- Advanced numerical simulation is needed for this study to enhance the understanding of PRF behavior and guide more effective designs.

Author Contributions: Conceptualization: F.A. and I.J., Methodology: F.A., I.J. and M.I.S., Experimental testing: M.I.S. and H.A.Q., Formal Analysis: M.I.S. and H.A.Q., Writing—original draft: M.I.S., H.A.Q. and F.A., Writing—review and editing: F.A., I.J., M.I.S. and H.A.Q. All authors have read and agreed to the published version of the manuscript.

Funding: This research received no external funding.

Data Availability Statement: The authors confirm that the data supporting the findings of this study are available within the article.

Acknowledgments: The researchers would like to thank the Deanship of Graduate Studies and Scientific Research at Qassim University for financial support (QU-APC-2024-9/1).

Conflicts of Interest: The authors declare no conflicts of interest.

References

1. Alnmr, A.; Ray, R.; Alzawi, M.O. Comparative Analysis of Foundation Systems in Expansive Soil: A Three-Dimensional Model Approach to Moisture Diffusion and Volume Changes. *Geotech. Geol. Eng.* **2024**, 1–27. [CrossRef]
2. Wang, G.; Zhang, X.; Liu, X.; Wang, H.; Xu, L.; Liu, H.; Peng, L. Soil arching effect in reinforced piled embankment for motor-racing circuit: Field tests and numerical analysis. *Transp. Geotech.* **2022**, *37*, 100844. [CrossRef]
3. Alsirawan, R.; Alnmr, A.; Koch, E. Experimental and Numerical Investigation of Geosynthetic-Reinforced Pile-Supported Embankments for Loose Sandy Soils. *Buildings* **2023**, *13*, 2179. [CrossRef]
4. Jamil, I.; Ahmad, I.; Rehman, A.U.; Siddiqi, M.I.; Ahmed, A.; Khan, A.M. Piles' load distribution in pile raft and pile group under lateral loading. *Mar. Georesources Geotechnol.* **2024**, *42*, 1034–1049. [CrossRef]
5. Swasdi, S.; Chub-Uppakarn, T.; Chompoorat, T.; Sae-Long, W. Numerical study on the influence of embedment footing and vertical load on lateral load sharing in piled raft foundations. *Geomech. Eng.* **2024**, *36*, 545–561.
6. Deb, P.; Pal, S.K. Structural and geotechnical aspects of piled raft foundation through numerical analysis. *Mar. Georesources Geotechnol.* **2022**, *40*, 823–846. [CrossRef]
7. Singh, H.; Tiwary, A.K. Analysis and Effect of Piles on Raft Foundation for High-Rise Framed Structure Under Seismic Loading. *Mater. Today Proc.* **2022**. [CrossRef]
8. Bazaz, H.B.; Akhtarpour, A.; Karamodin, A. A study on the effects of piled-raft foundations on the seismic response of a high rise building resting on clayey soil. *Soil Dyn. Earthq. Eng.* **2021**, *145*, 106712. [CrossRef]
9. Abdel-Azim, O.A.; Abdel-Rahman, K.; El-Mossallamy, Y.M. Numerical investigation of optimized piled raft foundation for high-rise building in Germany. *Innov. Infrastruct. Solut.* **2020**, *5*, 11. [CrossRef]
10. Rabiei, M.; Choobbasti, A.J. Piled Raft Design Strategies for High Rise Buildings. *Geotech. Geol. Eng.* **2016**, *34*, 75–85. [CrossRef]
11. Elsayed, T.; El-Shaib, M.; Gbr, K. Reliability of fixed offshore jacket platform against earthquake collapse. *Ships Offshore Struct.* **2016**, *11*, 167–181. [CrossRef]
12. Choo, Y.W.; Seo, J.-H.; Kim, Y.-N.; Goo, J.-M. Numerical Studies on Piled Gravity Base Foundation for Offshore Wind Turbine. *Mar. Georesources Geotechnol.* **2016**, *34*, 729–740. [CrossRef]
13. Yang, X.; Zeng, X.; Wang, X.; Yu, H. Performance of monopile-friction wheel foundations under lateral loading for offshore wind turbines. *Appl. Ocean. Res.* **2018**, *78*, 14–24. [CrossRef]
14. Doherty, P.; Spagnoli, G.; Doherty, M. Laboratory investigations to assess the feasibility of employing a novel mixed-in-place offshore pile in calcareous deposits. *Ships Offshore Struct.* **2020**, *15*, 29–38. [CrossRef]
15. Zeevaert, L. Compensated friction-pile foundation to reduce the settlement of buildings on the highly compressible volcanic clay of Mexico City. In Proceedings of the 4th International Conference on Soil Mechanics and Foundation Engineering, London, UK, 12–24 August 1957; pp. 81–86.
16. Viggiani, C.; Mandolini, A.; Russo, G. *Piles and Pile Foundations*; CRC Press: Boca Raton, FL, USA, 2014.
17. Siddiqi, M.I.; Jamil, I.; Hussain, M.A. Lateral Load Analysis of Piled Raft Foundation: A Review. *Tech. J.* **2024**, *3*, 584–590.
18. Jamil, I.; Ahmad, I.; Ullah, W. Contribution of raft to resist lateral loads in a piled raft foundation-experimental finding. *Earthq. Struct.* **2021**, *21*, 265–276.
19. Randolph, M. Design methods for pile group and piled rafts. In Proceedings of the 13th International Conference on SFE, New Dehli, India, 1 January 1994; pp. 61–82.
20. Poulos, H. Analysis of the settlement of pile groups. *Geotechnique* **1968**, *18*, 449–471. [CrossRef]
21. Burland, J.B.; Broms, B.B.; De Mello, V.F. Behaviour of foundations and structures. In Proceedings of the 9th International Conference on Soil Mechanics and Foundation Engineering, Tokyo, Japan, 10–15 July 1978.
22. Mandolini, A.; Russo, G.; Viggiani, C. Pile foundations: Experimental investigations, analysis and design. In Proceedings of the International Conference on Soil Mechanics and Geotechnical Engineering, Osaka, Japan, 12–16 September 2005; p. 177.
23. Lee, J.; Prezzi, M.; Salgado, R. Experimental investigation of the combined load response of model piles driven in sand. *Geotech. Test. J.* **2011**, *34*, 653–667. [CrossRef]
24. Bralović, N.; Despotović, I.; Kukaras, D. Experimental Analysis of the Behaviour of Piled Raft Foundations in Loose Sand. *Appl. Sci.* **2022**, *13*, 546. [CrossRef]
25. El-Garhy, B.; Galil, A.A.; Youssef, A.-F.; Raia, M.A. Behavior of raft on settlement reducing piles: Experimental model study. *J. Rock Mech. Geotech. Eng.* **2013**, *5*, 389–399. [CrossRef]
26. Kumar, V.; Kumar, A. An experimental study to analyse the behaviour of piled-raft foundation model under the application of vertical load. *Innov. Infrastruct. Solut.* **2018**, *3*, 35. [CrossRef]
27. Nguyen, D.D.C.; Jo, S.-B.; Kim, D.-S. Design method of piled-raft foundations under vertical load considering interaction effects. *Comput. Geotech.* **2013**, *47*, 16–27. [CrossRef]
28. Huang, M.; Liang, F.; Jiang, J. A simplified nonlinear analysis method for piled raft foundation in layered soils under vertical loading. *Comput. Geotech.* **2011**, *38*, 875–882. [CrossRef]
29. Jamil, I.; Ahmad, I.; Khan, I.; Ullah, W.; Rehman, A.U.; Khan, S.A. Factors affecting the lateral contribution of a raft in a piled raft system. *Ain Shams Eng. J.* **2023**, *14*, 101968. [CrossRef]
30. Deb, P.; Pal, S.K. Nonlinear analysis of lateral load sharing response of piled raft subjected to combined VL loading. *Mar. Georesources Geotechnol.* **2021**, *39*, 994–1014. [CrossRef]

31. Unsever, Y.; Matsumoto, T.; Özkan, M. Numerical analyses of load tests on model foundations in dry sand. *Comput. Geotech.* **2015**, *63*, 255–266. [CrossRef]
32. Horikoshi, K.; Matsumoto, T.; Hashizume, Y.; Watanabe, T.; Fukuyama, H. Performance of piled raft foundations subjected to static horizontal loads. *Int. J. Phys. Model. Geotech.* **2003**, *3*, 37–50. [CrossRef]
33. *ASTM Standard (D6913)*; Standard Test Methods for Particle-Size Distribution (Gradation) of Soils Using Sieve Analysis. ASTM International: West Conshohocken, PA, USA, 2017. Available online: https://www.astm.org/d6913-04r09e01.html (accessed on 14 November 2024).
34. Ateş, B.; Şadoglu, E. Experimental and Numerical Investigation for Vertical Stress Increments of Model Piled Raft Foundation in Sandy Soil. *Iran. J. Sci. Technol. Trans. Civ. Eng.* **2022**, *46*, 309–326. [CrossRef]
35. *ASTM Standard (D4253)*; Standard Test Methods for Maximum Index Density and Unit Weight of Soils Using a Vibratory Table. ASTM International: West Conshohocken, PA, USA, 2019. Available online: https://www.astm.org/d4253-16e01.html (accessed on 14 November 2024).
36. *ASTM Standard (D4254)*; Standard Test Methods for Minimum Index Density and Unit Weight of Soils and Calculation of Relative Density. ASTM International: West Conshohocken, PA, USA, 2016. Available online: https://www.astm.org/d4254-16.html (accessed on 14 November 2024).
37. *ASTM Standard (D854)*; Standard Test Methods for Specific Gravity of Soil Solids by Water Pycnometer. ASTM International: West Conshohocken, PA, USA, 2023. Available online: https://www.astm.org/d0854-14.html (accessed on 14 November 2024).
38. *ASTM Standard (D3080)*; Standard Test Method for Direct Shear Test of Soils Under Consolidated Drained Conditions. ASTM International: West Conshohocken, PA, USA, 2012. Available online: https://www.astm.org/d3080-04.html (accessed on 14 November 2024).
39. Katzenbach, R.; Turek, J. Combined pile-raft foundation subjected to lateral loads. In Proceedings of the 16th International Conference on Soil Mechanics and Geotechnical Engineering, Osaka, Japan, 12–16 September 2005; IOS Press: Amsterdam, The Netherlands, 2005; pp. 2001–2004.
40. Hoffmann, K. *Practical Hints for the Installation of Strain Gages*; Hottinger Baldwin Messtechnik GmbH: Darmstadt, Germany, 1996; Volume 56.
41. Al-Salih, O.; Al-Abboodi, I. Assessment of a new pluviation system designed to prepare uniform samples of sand. *J. King Saud Univ.-Eng. Sci.* 2023, *in Press*. [CrossRef]
42. Khari, M.; Kassim, K.A.; Adnan, A. An Experimental Study on Pile Spacing Effects under Lateral Loading in Sand. *Sci. World J.* **2013**, *2013*, 734292. [CrossRef]
43. Alam, M.J.; Hossain, M.S.; Azad, A.K. Development of correlation between dynamic cone resistance and relative density of sand. *J. Civ. Eng. Inst. Eng. Bangladesh (IEB)* **2014**, *42*, 63–76.
44. Mohammadi, S.; Nikoudel, M.; Rahimi, H.; Khamehchiyan, M. Application of the Dynamic Cone Penetrometer (DCP) for determination of the engineering parameters of sandy soils. *Eng. Geol.* **2008**, *101*, 195–203. [CrossRef]